

Received September 16, 2020, accepted September 29, 2020, date of publication October 19, 2020, date of current version April 27, 2021.

Digital Object Identifier 10.1109/ACCESS.2020.3031903

# Energy Storage System Control Strategy for Restraining Overvoltage Caused by Switching Non-Load Power Transmission Lines

BO YANG, HAOJIE YU<sup>1</sup>, GUANJUN LI, ANPING HU<sup>1</sup>, AND HAOYUAN LI, (Member, IEEE)

China Electric Power Research Institute Company Ltd., Nanjing 210003, China

Corresponding author: Haojie Yu (yuhaojie@epri.sgcc.com.cn)

This work was supported by the National Key Research and Development Program of China under Grant 2018YFB0905500.

**ABSTRACT** During the switching operation of the non-load power transmission lines, the undesired switching overvoltage issue is inevitable, causing grid voltage oscillations, waveform distortion and other phenomena at the end of the non-load power transmission lines, and even lead to the insulation breakdown, all above phenomena probably make the power transmission failure. To avoid the above harmful cases, the formation mechanism of the undesired switching overvoltage issue caused by switching non-load power transmission lines is first analyzed in detail. Based on this mechanism analysis, the energy storage system (ESS) based overvoltage suppression method and corresponding ESS voltage command synthesis algorithm are developed. The method can quickly and effectively restrain the voltage change rate and reduce the voltage difference between the initial value and the steady state value of the power transmission lines, so that the line voltage during the switching operation can be kept within the safety limit range. Finally, a simulation model was built by using MATLAB/Simulink software, and the simulation results verified the effectiveness of the proposed overvoltage suppression strategy.

**INDEX TERMS** Switching overvoltage, energy storage system (ESS), non-load power transmission lines, voltage command synthesis algorithm.

## I. INTRODUCTION

As the proportion of renewable energy sources in the grid continues to increase, more and more renewable energy power plants are established in remote areas [1]. High-voltage and long-distance power transmission has become a necessary choice to collect such renewable energy power to the main power system. With the establishment and development of ultra-high-voltage (UHV) and long-distance power transmission lines, the probability of over-voltage on closed non-load power lines (including reclosing) is greater and more serious. During the switching operation of the non-load power transmission lines, a large switching overvoltage will be generated due to the effect of the huge line capacitance [2]. The switching overvoltage is several times higher than the rated voltage so that the oscillation, waveform distortion and even insulation breakdown will have probably occurred.

The associate editor coordinating the review of this manuscript and approving it for publication was Bin Zhou<sup>1</sup>.

All these phenomena probably made power transmission failure, so it must be suppressed in time [3].

Various strategies for restraining overvoltage caused by switching non-load power transmission lines have been reported and tested in existing literature. The shunt reactor is firstly adopted to suppress the power frequency overvoltage in [4], and it is validated that the shunt reactor method can effectively suppress the amplitude and duration of the switching overvoltage [5]. However, this method is mainly focused on the suppression of the power frequency overvoltage, therefore, it has no obvious effect on the oscillating overvoltage of the transmission process. To this end, the series compensation capacitor method is therefore presented in [6-7], and their simulation results showed that the switching overvoltage can be suppressed to some extent. But the method still cannot meet the overvoltage reference standard of the ultra-high voltage operating and hence, it can only be used as the auxiliary method. In [8], the switching resistor is utilized in the circuit breaker to suppress the overvoltage. In [9], to effectively improve the above method, the pre-insertion

resistor scheme is presented to substitute the switching resistor. But in any case, the above methods should well address the following problems, such as the complex hardware structure, expensive hardware price, low reliability, high maintenance fee and so on. Afterwards, in [10], Eiichi Zaima proposed the switching overvoltage control strategy via the application of surge arresters and circuit breakers with closing/opening resistors in 1100 kV substations and power transmission lines. In [11], X. Kou analyzed Henan power circuit breakers with closing resistors operation, and switching overvoltage and surge arrester energy absorption were simulated without the closing resistor for a typical substation. However, they have not put forward any effective methods or strategies to decrease and suppress the undesired switching overvoltage. In [12], the phase-controlled switching method, which will control the circuit breaker to complete the circuit switching at a specified phase, was proposed and it is verified that the phase-controlled switching method is effective enough, and it can get more enough suppression effect when it is combined with other methods. However, the disadvantage of this method is that it cannot realize the three phases switching at the same time, so that the overcurrent issue may be produced. In addition, this method needs a high precision circuit breaker and controller, therefore it is difficult to be well implemented. The metal oxide arrester (MOA) is also employed to suppress the switching overvoltage [13], and their research results showed that the overvoltage at every point of the power transmission line can be limited under 2.0 p.u. If both the MOA and the switching resistor are used at the same time, the desired coordinated operation can be achieved, i.e. MOA can suppress the overvoltage low enough after the switching resistor is shorted. However, if the resonant overvoltage has a high amplitude and a long duration, the MOA will be damaged because it absorbed too much energy. For the overvoltage caused by the three-phase simultaneous breaking operation, the phase-controlled switching strategy based on fast vacuum switch is proposed in [14], which uses the fast vacuum switch and phase-controlled switching technology, which is effective for the breaking overvoltage. In UHV power systems, J. L. He and B. Han proposed the closing resistors for breakers to suppress the switching overvoltage, besides, the different arresters, like controllable surge arrester (CSA), was used to eliminate the closing resistor of circuit breakers. But their shortcomings make it a long-standing goal to eliminate closing resistors. The main factors that effect the close overvoltage are analyzed, and the results demonstrated that the amplitudes of the switching overvoltage were mainly related to the close phase angles with its range from 1.17p.u to 2.14p.u., which is useful to look for the best close phase angles. Compared with the above suppression methods, the energy storage system (ESS) based methods have the incomparable characteristics that it not only can realize the fast suppression for the switching overvoltage, but also can be well implemented easily. Based on the ESS application, the corresponding ESS voltage command synthesis algorithm is developed. This method can quickly and effectively restrain

the voltage change rate and reduce the voltage difference between the initial value and the steady state value of the power transmission lines, so that the line voltage during the switching operation can be kept within the safety limit range. The simulation results verified the effectiveness of the proposed method.

The remainder of this paper is organized as follows. Section II analyses the mechanism of circuit closing overvoltage. Then, The principle of ESS suppressing non-load closing overvoltage is analyzed in Section III. The ESS control strategy is proposed in Section IV. Simulation verification is confirmed in Section V. The conclusions are drawn in Section VI.

## II. MECHANISM OF SWITCHING OVERVOLTAGE ISSUES

The switching overvoltage will be generated when the non-load power transmission line is powered.

It is assumed that the three phases of the circuit breaker are completely operated at the same time, then the sum of the forced component and the transient component of the three phases on the transmission line are all zero. The voltage during the transition process only depends on the positive sequence parameters, so the single phase non-load closed loop can be used to analysis the switching overvoltage.

As shown in Fig.1,  $e(t)$  is the power supply voltage;  $X_s$  is the inner impedance of the power supply; QF is the circuit breaker;  $E$  is the amplitude of the power supply voltage;  $U_2$  is the power frequency voltage amplitude at the end of the non-load power transmission line.

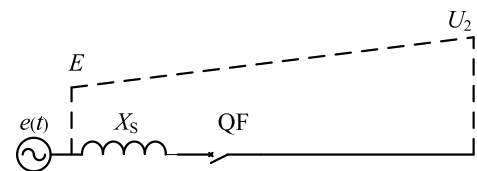


FIGURE 1. The diagram for studying the switching overvoltage of the non-load power transmission line.

The switching process of the non-load long transmission line can be equivalent to a series T-equivalent circuit with an equivalent inductor and a equivalent capacitor as shown in Fig.2 [12]. Here,

$$L = 1/3L_0l \quad (1)$$

$$C = C_0l \quad (2)$$

where,  $L$  and  $C$  is the equivalent inductance and capacitance of the non-load power transmission line, respectively.  $C_0$  is the inductance and capacitance of the unit length line, respectively.  $l$  is the transmission line length between the measuring point and the power supply.

Neglecting the equivalent resistances of the power supply and the power transmission line, the system can be equivalent to an infinity power supply before switching on, then the voltage of the power supply can be expressed as:

$$e(t) = E_m \sin(\omega t + \varphi) \quad (3)$$

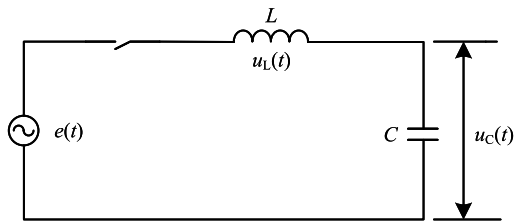


FIGURE 2. The T-type equivalent circuit of the non-load long transmission line during switching process.

where  $E_m$  is the amplitude of the power supply voltage,  $\omega$  is the angle frequency of the power supply voltage;  $\varphi$  is the initial phase, respectively.

According to the Kirchhoff voltage law, we have

$$e(t) = u_L(t) + u_C(t) \tag{4}$$

The above circuit equation can be expressed as

$$e(t) = LC \frac{d^2 u_C(t)}{dt^2} + u_C(t) \tag{5}$$

Then, the voltage on the capacitor can be expressed as

$$\begin{aligned} u_C(t) &= E_m \sin \varphi (1 - \cos \omega_0 t) \tag{6} \\ u_C &= E_m \sin \varphi (1 - \cos \omega_0 t) \\ &+ \int_0^t \omega E_m \cos(\omega \tau + \varphi) [1 - \cos \omega_0 (t - \tau)] d\tau \\ &= E_m \frac{\omega_0^2}{\omega_0^2 - \omega^2} \sin(\omega t + \varphi) \\ &- E_m \frac{\omega_0^2}{\omega_0^2 - \omega^2} \sqrt{\sin^2 \varphi + \left(\frac{\omega}{\omega_0} \cos \varphi\right)^2} \\ &\times \sin(\omega_0 t + \psi) \tag{7} \end{aligned}$$

To get the accurate switching overvoltage value, Duhamel integral is utilized in this paper. The voltage is decomposed into a number of step functions with an time interval, and the solution of each step function is superimposed, then the voltage on the capacitor can be expressed as Eq.(7), where

$$\begin{aligned} \omega_0 &= \frac{1}{\sqrt{LC}} \\ \psi &= \tan^{-1} \frac{\omega_0 \sin \varphi}{\omega \cos \varphi} \end{aligned}$$

Therefore, the maximum value of the capacitor voltage can be expressed as

$$(u_C)_m = E_m \left| \frac{\omega_0^2}{\omega_0^2 - \omega^2} \right| \left[ 1 + \sqrt{\sin^2 \varphi + \left(\frac{\omega}{\omega_0} \cos \varphi\right)^2} \right] \tag{8}$$

It is relevant with the phase angle of the AC power supply switching. If  $\varphi = 90^\circ$ , the switching operation is conducted when the power supply voltage reached the maximum value. Then, the switching overvoltage reached the maximum value

as the following

$$(u_C)_m = 2E_m \left| \frac{\omega_0^2}{\omega_0^2 - \omega^2} \right| = 2E_m \left| \frac{1}{1 - \left(\frac{\omega}{\omega_0}\right)^2} \right| \tag{9}$$

Compared with the switching of the single phase long non-load transmission line, the overvoltage problem of the three phases is more complicated, but the analysis methods are completely identical.

Since the three phase voltages are  $120^\circ$  out of phase, so at least two phases are in the overvoltage state at any time on the non-load long transmission line, and the overvoltage exhibits AC oscillating characteristics.

### III. PRINCIPLE OF ESS SUPPRESSING THE SWITCHING OVERVOLTAGE

Fig.3 shows the principle of the ESS based switching overvoltage suppressing schematic, and ESS is installed in parallel with the circuit breaker.

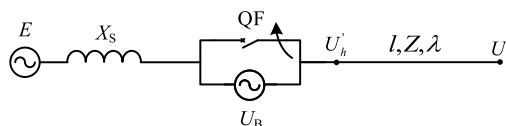


FIGURE 3. The principle of ESS suppressing the switching overvoltage.

Assumed that the frequency and phase of the output voltage of the ESS are in accord with the power supply voltage, and its amplitude decreases with time via a certain slope  $h$ , then at the  $t_1$  moment, the steady state voltage at the head of the transmission line can be expressed as

$$\dot{U}'_{h1} = \dot{E} - (\dot{E} - ht_1) = ht_1 \tag{10}$$

Accordingly, the voltage at the terminal of the transmission line can be calculated as

$$\dot{U}_{e1} = \frac{\dot{U}'_{h1}}{\cos \lambda} = \frac{ht_1}{\cos \lambda} \tag{11}$$

After the  $dt$  time, the steady state voltage at the head of the transmission line can be calculated as

$$\dot{U}'_{h2} = h(t_1 + dt) \tag{12}$$

Accordingly, the end voltage of the transmission line can be expressed as

$$\dot{U}_{e2} = \frac{\dot{U}'_{h2}}{\cos \lambda} = \frac{h(t_1 + dt)}{\cos \lambda} \tag{13}$$

As shown above, during the  $dt$  time interval, the steady state voltage at the terminal of the transmission line is oscillating and changing from  $\dot{U}_{e1}$  to  $\dot{U}_{e2}$ . If the voltage phase angle is  $\alpha$  at  $t_1$  moment, then the steady state value of the oscillation process can be expressed as

$$U_{st} = \sqrt{2}U_{e2} \sin(\alpha + \omega dt) \tag{14}$$

Here, the initial voltage can be expressed as

$$U_{be} = \sqrt{2}U_{e1} \sin \alpha \quad (15)$$

Then, the amplitude of the free oscillation component during the transition can be expressed as

$$U_a = U_{st} - U_{be} = \sqrt{2}U_{e2} \sin(\alpha + \omega dt) - \sqrt{2}U_{e1} \sin \alpha \quad (16)$$

When the  $dt$  is small enough, it holds

$$\sin(\alpha + \omega dt) = \sin \alpha$$

Therefore, the amplitude of the free oscillation component can be calculated as

$$U_a = \sqrt{2}U_{e2} \sin \alpha - \sqrt{2}U_{e1} \sin \alpha = \sqrt{2} \frac{hdt}{\cos \lambda} \sin \alpha \quad (17)$$

During the transition process, the amplitude of the free oscillating voltage is much smaller than the steady-state voltage amplitude.

Therefore, when the frequency and phase of the output voltage of the ESS is in accord with the power supply voltage, and its amplitude decreases with time via a certain slope  $h$ , the switching overvoltage can be suppressed effectively. When the output voltage of the ESS is decreased to  $\theta$ , the ESS can be shorted, and the non-load power transmission line started to work normally.

#### IV. ESS CONTROL STRATEGY FOR RESTRAINING THE SWITCHING OVERVOLTAGE

To realize the above operation goals, the ESS should be controlled as follows.

The amplitude of the head voltage of the non-load power transmission line rise with a certain slope till to the amplitude of the power grid sinusoidal voltage, and the phase follows the power grid voltage phase, then the ESS output voltage  $U_{Bref}$  is the difference between the power grid voltage and the head voltage of the non-load power transmission line, which gives

$$U_{Bref} = U(t) \sin(\omega t + \varphi) \quad (18)$$

where  $U(t)$  is a command function of the ESS voltage amplitude.

##### A. ESS VOLTAGE COMMAND SYNTHESIS METHOD

After the amplitude and phase of the output voltage of the ESS is determined, its voltage command can be quickly synthesized as shown in Fig.4. The synthesized process of the voltage amplitude and phase is expressed as following.

##### 1) PHASE INSTRUCTION

The frequency and phase of the non-load power transmission line head voltage are in accord with the power supply voltage, so the phase and frequency of the ESS output voltage must be identical with that of the power grid.

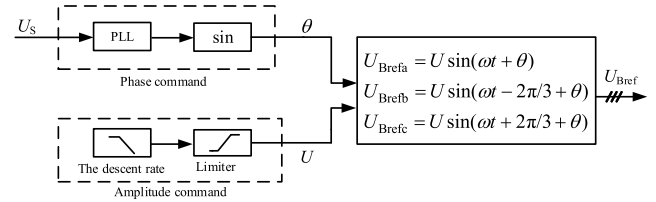


FIGURE 4. The voltage command synthesis method of ESS.

Then, the phase command  $\theta(t)$  of the power grid current can be expressed as

$$\theta(t) = \omega t + \alpha \quad (19)$$

However, the phase of the power grid voltage is always changing in real time. In order to ensure that the voltage phase always satisfies (19), the grid voltage phase detection method is used to track the phase in real time.

The phase detection method of the power grid voltage has two categories [5]–[7], i.e. open-loop phase measurement and closed-loop phase measurement. In this paper, the typical closed-loop phase measurement method, i.e. the single synchronous frame based phase locked loop (PLL) method, is adopted, as shown in Fig.5. The coordinate transformation between Cartesian  $abc$  and plane coordinate system  $\alpha\beta$  adopted in Fig.5 can be expressed as

$$\begin{bmatrix} u_\alpha \\ u_\beta \end{bmatrix} = \sqrt{\frac{2}{3}} \begin{bmatrix} 1 & -\frac{1}{2} & -\frac{1}{2} \\ 0 & \frac{\sqrt{3}}{2} & -\frac{\sqrt{3}}{2} \end{bmatrix} \begin{bmatrix} u_{sa} \\ u_{sb} \\ u_{sc} \end{bmatrix} \quad (20)$$

$$\begin{bmatrix} u_d \\ u_q \end{bmatrix} = \frac{2}{3} \begin{bmatrix} \cos \theta & \sin \theta \\ -\sin \theta & \cos \theta \end{bmatrix} \begin{bmatrix} u_\alpha \\ u_\beta \end{bmatrix} \quad (21)$$

where  $\theta$  is the phase of the power grid voltage calculated by the PLL shown in Fig.5.

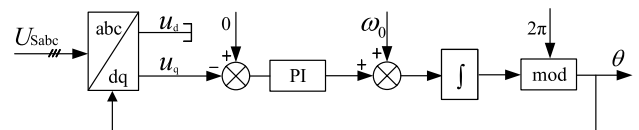


FIGURE 5. The control block diagram of the PLL.

##### 2) AMPLITUDE INSTRUCTION

Constraints condition on the magnitude of the output voltage of the ESS is that the head voltage of the power transmission line is sinusoidal whose amplitude rises to the power grid voltage amplitude with a certain slope, so the amplitude of the output voltage of ESS should reduce from the power grid voltage amplitude till zero at a certain slope.

The slope of the voltage amplitude drop should not be too small to ensure that the transmission line can work at a stable state as soon as possible. Simultaneously, according to the (17), the slope of the voltage amplitude drop should not be too strong to avoid the voltage oscillation. Therefore,

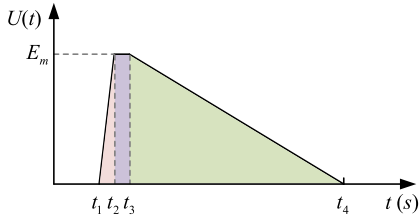


FIGURE 6. The voltage amplitude slope of ESS.

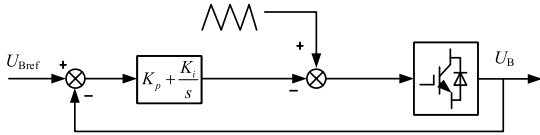


FIGURE 7. The direct voltage tracking control of ESS.

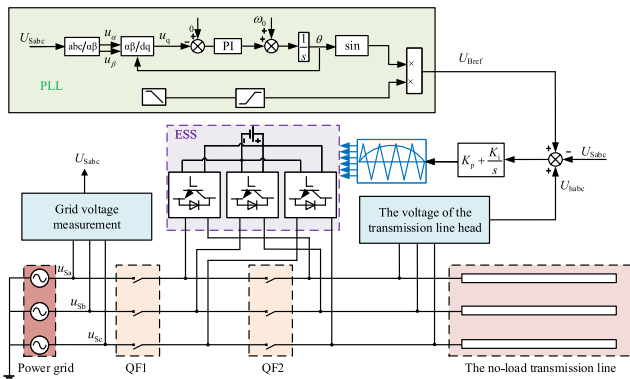


FIGURE 8. The system structure diagram and the ESS control system.

the falling slope of the voltage amplitude needs to be kept within a reasonable range as shown in Fig.6.

According to the above analysis, the amplitude command of the power grid can be expressed as

$$U(t) = \begin{cases} 0 & t < t_1 \\ k_r(t - t_1) & t_1 < t < t_2 \\ E_m & t_2 < t < t_3 \\ E_m - k_d(t - t_3) & t_3 < t < t_4 \\ 0 & t < t_4 \end{cases} \quad (22)$$

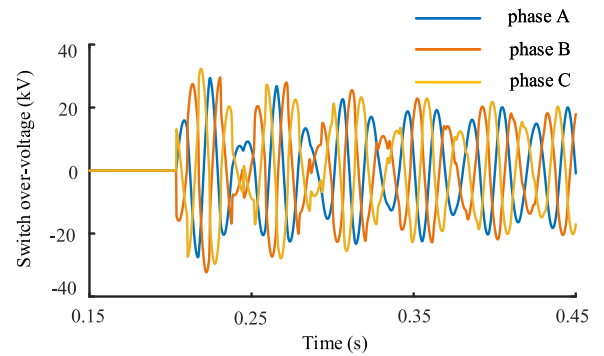
Here,  $E_m$  is the voltage amplitude of the power grid;  $k_r$  is the rise rate of the output voltage of ESS, which is affected by the output voltage of ESS on the following ability of the command signal;  $k_d$  is the decline rate of the output voltage of ESS, which is affected by the control strategy;  $t_1$  is the preparatory closing moment;  $t_2$  is the closing moment;  $t_3$  is the moment when the output voltage of ESS starts to decline;  $t_4$  is the short-circuit moment of ESS. The above time parameters satisfy the following relationship, i.e.

$$t_2 - t_1 > \frac{1}{k_r} E_m \quad (23)$$

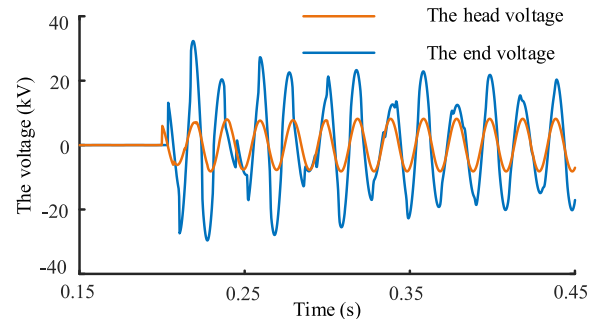
$$t_4 = t_3 + \frac{1}{k_d} E_m \quad (24)$$

TABLE 1. The main parameters.

Symbol	Description	value
$t_1$	The switching time of the non-load power line	0.2 s
$f$	The frequency of the grid voltage and current	50 Hz
$U_s$	The amplitude of the power grid voltage	10 kV
$R_0$	The unit resistance of the transmission line	0.012 $\Omega$ /km
$L_0$	The unit inductance of the transmission line	0.9 mH/km
$C_0$	The unit capacitance of the transmission line	1.2 nF/km
$K_p$	The proportional coefficient of the PI controller	100
$K_i$	The integral coefficient of the PI controller	500
$K_d$	The decrease rate of the ESS voltage	50 kV/s



(a) Switching overvoltage



(b) oltage comparison between the terminal and end of phase C

FIGURE 9. The closing overvoltage without any suppression strategy.

Therefore, the real-time ESS voltage command value can be determined according to (19) and (21).

### B. ESS CONTROL METHOD

To suppress the switching overvoltage, the control strategy must have the rapid response ability. Therefore, the direct voltage tracking control method in the abc coordinate system is adopted to realize the ESS voltage command tracking in the paper, as shown in Fig.7. Here, the classic PI controller is adopted as the loop compensator. In addition,  $k_p$  and  $k_i$  are the proportional and integral coefficients of the adopted PI controller, respectively.

If the measured output voltage of the ESS is  $U_B$ , the modulation signal of the ESS inverter can be obtained by

$$u_{Bref} = K_p (U_{Bref} - U_B) + K_i \int (U_{Bref} - U_B) dt \quad (25)$$

Integrating the above-mentioned voltage command synthesis method, inverter circuit, ESS control strategy and power

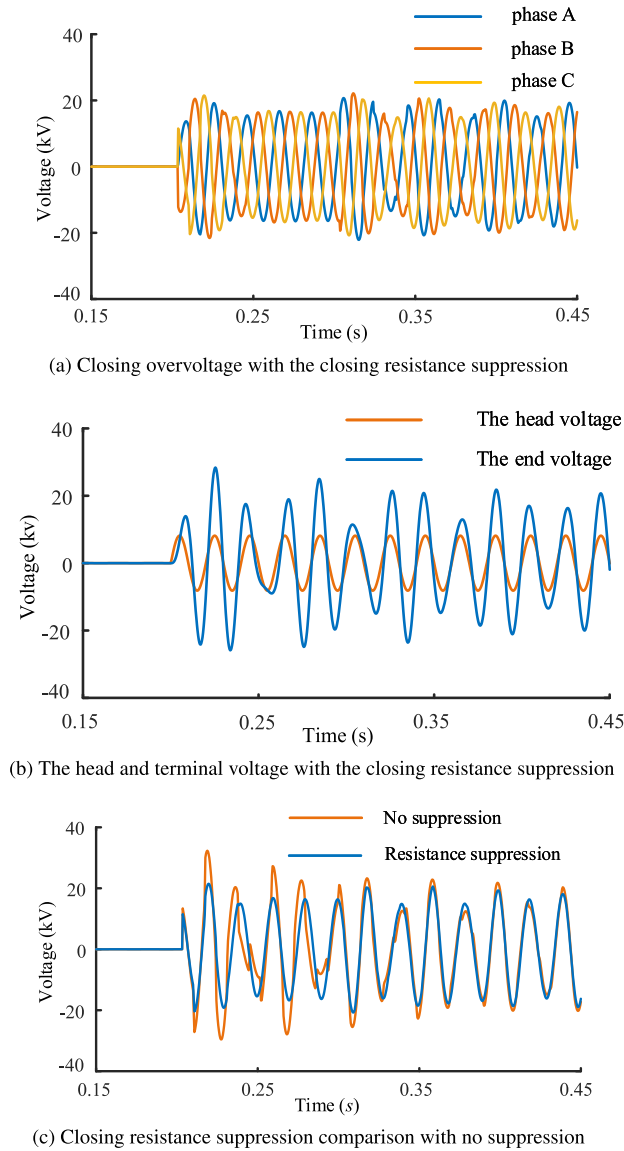


FIGURE 10. Diagram of closing overvoltage with suppression strategy.

grid voltage phase detection method, the panoramagram of the ESS based switching overvoltage suppression method can be obtained, as shown in Fig.8. Where,  $U_{Sabc}$  is the voltage of the power grid;  $U_{Bref}$  is the voltage command of the ESS;  $U_{habc}$  is the measured voltage value at the head of the non-load transmission line.

V. SIMULATION VERIFICATION

The simulation model of the non-load power transmission line is built by the MATLAB/Simulink to reproduce the switching overvoltage phenomenon and to verify the corresponding suppression strategy. The simulation results are shown in Fig.9-Fig.12. The main parameters of the simulation model are shown in Tab.1.

As shown in Fig. 9(a), the switching overvoltage in the non-load power transmission line is generated when there

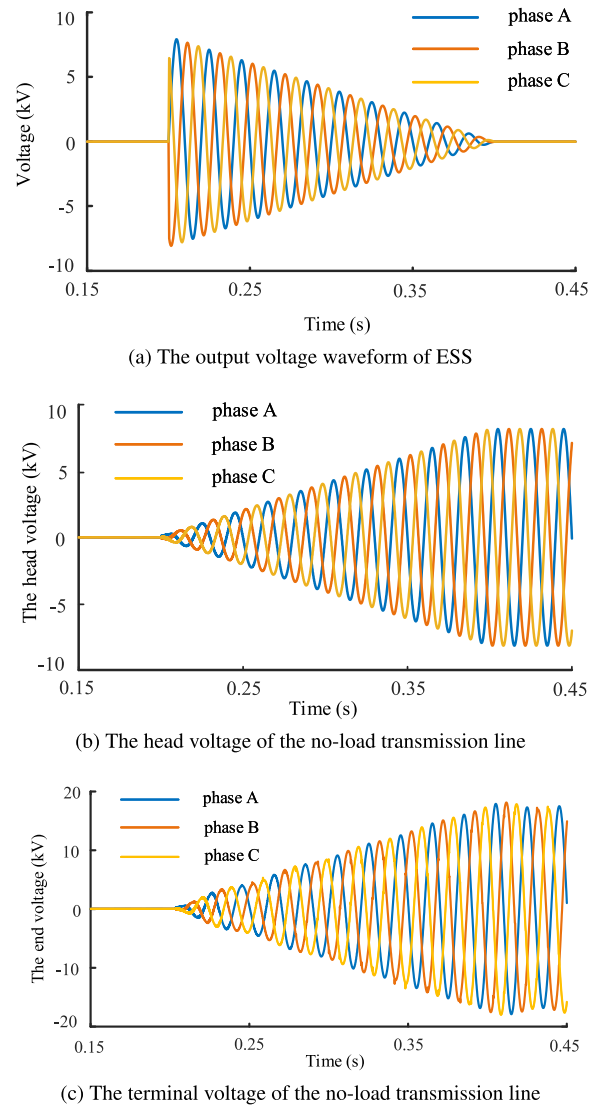


FIGURE 11. The voltage waveform with ESS.

is not any suppression device or any control strategy. The switching overvoltage at the terminal of the non-load transmission line is the most serious, and the maximum amplitude of the overvoltage can reach 1.9 times of the power supply voltage, and such high overvoltage can make the insulation of the transmission line breakdown. The switching overvoltage decreases till to the power frequency voltage within the 0.5 s. Fig.9 (b) shows switching overvoltage at the head and terminal of the single phase non-load transmission line.

Fig.10(a) shows the overvoltage suppression effect with the closing resistance. It can be seen that the overvoltage is suppressed at some extent. However, as shown in Fig.10(b), the head voltage occurs two steps, it is respectively the moment of the resistance connected and exited from the transmission line, i.e. 0.2 s and 0.3 s, accordingly the terminal voltage occurs two oscillations. The maximum amplitude of the terminal voltage is about 1.3 times of the power frequency

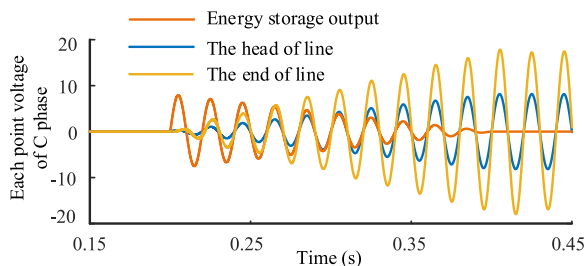
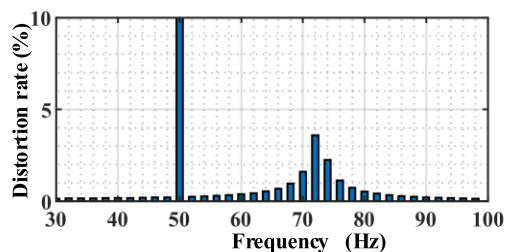
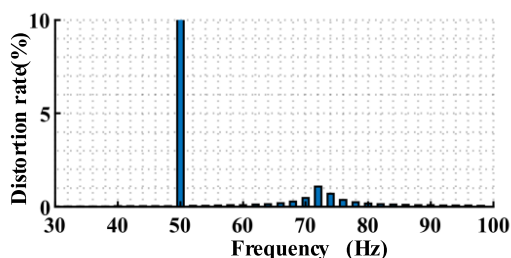


FIGURE 12. The voltage waveform with ESS.



(a) without any control strategy



(b) with ESS

FIGURE 13. The voltage harmonic at the steady state based on the Fourier analysis.

voltage, and it is smaller than the overvoltage amplitude without any suppression device or strategy, the comparison results are shown in Fig.10(c).

When ESS is connected to the transmission line, the output voltage is shown in Fig.11(a). It can be seen that the amplitude of the voltage is decreasing at a certain slope till to zero, and then stop the operation of the ESS.

To clearly observe the effect of the ESS on the overvoltage suppression, phase C is selected to show the voltage change trend, as shown in Fig.12. It can be seen that the non-load power transmission line head overvoltage disappears with the help of the ESS. The phase difference between the steady state value and the initial value is small enough, and accordingly the free oscillation voltage is also small so that it is negligible compared with the overvoltage generated without suppression device.

Comparing the results in Fig. 9(b) and Fig. 12, it can be found that when there is no suppression strategy, it needs about 0.3 s to reach the steady state value for the non-load power transmission line terminal voltage. However, it only needs 0.2 s when the ESS is connected to the non-load power transmission line.

Fourier analysis is performed after 0.5 s when the terminal voltage reached the steady state, the results are shown in Fig.13. It can be found that the harmonic distortion rate is 5.13% when there is no suppression strategy, the harmonic distortion rate is 3.56% when the switching resistor is used, and the harmonic distortion rate is 1.55% when ESS is utilized. The above results showed that the ESS based overvoltage suppression strategy for the non-load power transmission line can also shorten the time that the line enters the stable operating state, and reduce the harmonic distortion rate of the line voltage.

## VI. CONCLUSION

The ESS based overvoltage suppression strategy for the non-load power transmission line is proposed, and the simulation results showed that it can realize the following purpose:

- (1) Follow the line voltage rapidly and ensure that there is no severe voltage step at the head of the non-load power transmission line;
- (2) Ensure that the end of the non-load transmission line will not produce a serious non-load switching overvoltage;
- (3) Shorten the time that the non-load power transmission line reaches the steady state voltage;
- (4) Reduce the harmonic distortion rate of the terminal voltage of the non-load power transmission line.

## REFERENCES

- [1] L. Xiong, F. Zhuo, X. Liu, Z. Xu, and Y. Zhu, "Fault-tolerant control of CPS-PWM-based cascaded multilevel inverter with faulty units," *IEEE J. Emerg. Sel. Topics Power Electron.*, vol. 7, no. 4, pp. 2486–2497, Dec. 2019.
- [2] W. Binbing, X. Abuduwayiti, C. Yuxi, and T. Yizhi, "RoCoF droop control of PMSG-based wind turbines for system inertia response rapidly," *IEEE Access*, vol. 8, pp. 181154–181162, 2020.
- [3] L. Xiong, F. Zhuo, F. Wang, X. Liu, Y. Chen, M. Zhu, and H. Yi, "Static synchronous generator model: A new perspective to investigate dynamic characteristics and stability issues of grid-tied PWM inverter," *IEEE Trans. Power Electron.*, vol. 31, no. 9, pp. 6264–6280, Sep. 2016.
- [4] L. Xiu, Z. Du, M. Li, L. Du, J. Hao, and Z. Kang, "A practical and fast sequence components detection scheme for three-phase unbalanced grid voltage," *Int. J. Elect. Power Energy Syst.*, vol. 125, Feb. 2021, Art. no. 106385.
- [5] L. Xiong, X. Liu, C. Zhao, and F. Zhuo, "A fast and robust real-time detection algorithm of decaying DC transient and harmonic components in three-phase systems," *IEEE Trans. Power Electron.*, vol. 35, no. 4, pp. 3332–3336, Apr. 2020.
- [6] L. Xiong, F. Zhuo, F. Wang, X. Liu, and M. Zhu, "A fast orthogonal signal-generation algorithm characterized by noise immunity and high accuracy for single-phase grid," *IEEE Trans. Power Electron.*, vol. 31, no. 3, pp. 1847–1851, Mar. 2016.
- [7] B. Wu, Y. Tian, Y. Chen, X. Abuduwayiti, and L. Xiong, "Virtual frequency construction based vector current control for grid-tied inverter under imbalanced voltage," *IEEE Access*, early access, Oct. 13, 2020, doi: 10.1109/ACCESS.2020.3030648.
- [8] L. Wang, X. Zhou, Y. Huang, Y. Wang, Y. Li, and J. Huang, "Simulation study on restrain strategy for no-load switching overvoltage of UHV transmission line," in *Proc. IEEE/IAS Ind. Commercial Power Syst. Asia (I&CPS Asia)*, Weihai, China, Jul. 2020, pp. 397–401.
- [9] H. Seyedi, S. Golabi, and Z. Abam, "Limitation of transmission line switching overvoltages," in *Proc. IEEE Int. Conf. Power Energy*, Kuala Lumpur, Malaysia, Nov. 2010, pp. 363–368.
- [10] E. Zaima, "System aspects of 1100 kV AC transmission technologies in Japan," *IEEJ Trans. Electr. Electron. Eng.*, vol. 4, no. 1, pp. 62–66, Jan. 2009.

- [11] X. Kou, "Study on dismantling the closing resistor of 500kV breaker in Henan power grid," in *Proc. Int. Conf. E-Product E-Service E-Entertainment*, Nov. 2010, pp. 1–4.
- [12] S. W. Shu and C. Liu, "Simulation research on limit of closing overvoltage by phase controlled technology in 1000kV transmission lines," *Elect. Technol.*, vol. 15, no. 1, pp. 27–32, Nov. 2016.
- [13] F. J. Guo, H. P. Xue, and H. Y. Xu, "Research on the replacing the closing resistor with the MOA applied in the ultra high pressure transmission," *Electrotech. Appl.*, vol. 10, no. 34, pp. 71–74, Nov. 2015.
- [14] Z. Huang, W. Tan, Q. Mao, L. Zou, and J. Zou, "Controlled breaking strategy of shunt reactor based on fast vacuum switch," in *Proc. 5th Int. Conf. Electr. Power Equip.-Switching Technol. (ICEPE-ST)*, Kitakyushu, Japan, Oct. 2019, pp. 670–698.



**BO YANG** is currently pursuing the master's degree. He is a Researcher-Level Senior Engineer, the Director of the Energy Storage Application Technology Research Office, China Electric Power Research Institute Company Ltd., New Energy Research Center, and an Executive Deputy Director with the Jiangsu Energy Storage Conversion and Integrated Application Engineering Technology Research Center. He is also a Professional Leading Talent with the State Grid Corporation and the 333 Third-Level Talents in Jiangsu Province. He has a number of major national, provincial, and state grid company science and technology projects. He has a national standard. He has published 14 EI search articles. His research interests include energy storage conversion technology research, energy storage system application integration, distributed power generation, microgrid technology research, and system integration application work. He received two first prizes and two second prizes for scientific and technological progress from the State Grid Corporation and four provincial and ministerial awards.



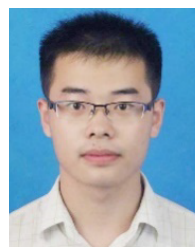
**HAOJIE YU** is currently pursuing the master's degree. He is currently an Engineer with the Energy Storage Application Technology Research Office, New Energy Research Center, China Electric Power Research Institute Company. He has participated with the development of energy storage converters with different power levels of 30-500kVA, the development of DC/DC converters, and the construction of energy storage conversion and application technology laboratories. He has also participated with the National Key Research and Development Project, MW-Level Advanced Flywheel Energy Storage Key Technology Research, and the State Grid Corporation's Science and Technology Project, Distributed New Energy Power Generation System Grid Connection and Dispatch Operation Key Technology Research and Engineering Demonstration Projects, and obtained authorization. He holds five patents. He received the First Prize from the National Electric Power Workers Technical Achievement Award, the Second Prize from the State Grid Corporation of Science and Technology Progress, and the Third Prize from the State Grid Electric Power Research Institute Science and Technology Progress Award. This project undertakes the research of multidevice parallel coordinated control technology.



**GUANJUN LI** is currently pursuing the master's degree. He is also a Senior Engineer. He has published 16 core articles. He holds 14 patents. His main research interests include energy storage converter control technology, distributed power generation, and microgrid and other directions. He received one first prize and one second prize from the State Grid Science and Technology Progress Award and one Third Prize from the State Grid Patent.



**ANPING HU** received the B.Sc. degree in automation from the Zhengzhou University of Light Industry, Zhengzhou, China, in 2006, the M.A.Sc. degree in power electronics from Guizhou University, Guizhou, China, in 2009, and the Ph.D. degree in electrical engineering from the Hefei University of Technology, Hefei, China, in 2015. From 2011 to 2013, he was a Visiting Ph.D. Student with Ryerson University, Toronto, ON, Canada. He is currently with the China Electric Power Research Institute Company as a Senior Engineer. His research interests include power systems, energy storage system and application, power converter systems, and power quality of renewable energy systems.



**HAOYUAN LI** (Member, IEEE) received the B.S. and Ph.D. degrees in electrical engineering and automation from the Hefei University of Technology, Hefei, China, in 2013 and 2019, respectively. Since 2019, he has been with China Electric Power Research Institute Company Ltd., as a Research and Development Engineer and a Project Manager. His main research interests include energy storage converter control technology, synchronous motor control technology, and high-power power electronic converter technology.

...